Talanta 116 (2013) 801–808

Contents lists available at ScienceDirect

Talanta

journal homepage: www.elsevier.com/locate/talanta

A high-performance glucose biosensor using covalently immobilised glucose oxidase on a poly(2,6-diaminopyridine)/carbon nanotube electrode

Mohammad Ali Kamyabi [a,b,*], Nasim Hajari [b], Anthony P.F. Turner [a], Ashutosh Tiwari [a,*]

[a] Biosensors and Bioelectronics Centre, Department of Physics, Chemistry and Biology, IFM-Linköping University, S-58183 Linköping, Sweden
[b] Department of Chemistry, Faculty of Sciences, University of Zanjan, P.O. Box 45195-313, Zanjan, Islamic Republic of Iran

ARTICLE INFO

Article history:
Received 21 May 2013
Received in revised form
25 July 2013
Accepted 26 July 2013
Available online 3 August 2013

Keywords:
Glucose biosensor
Direct electron transfer
Glucose oxidase
MWNT/poly-(2,6-diaminopyridine)

ABSTRACT

A highly-sensitive glucose biosensor amenable to ultra-miniaturisation was fabricated by immobilisation of glucose oxidase (GOx), onto a poly(2,6-diaminopyridine)/multi-walled carbon nanotube/glassy carbon electrode (poly(2,6-DP)/MWNT/GCE). Cyclic voltammetry was used for both the electrochemical synthesis of poly-(2,6-DP) on the surface of a MWNT-modified GC electrode, and characterisation of the polymers deposited on the GC electrode. The synergistic effect of the high active surface area of both the conducting polymer, i.e., poly-(2,6-DP) and MWNT gave rise to a remarkable improvement in the electrocatalytic properties of the biosensor. The transfer coefficient (α), heterogeneous electron transfer rate constant and Michaelis–Menten constant were calculated to be 0.6, 4 s^{-1} and 0.20 mM at pH 7.4, respectively. The GOx/poly(2,6-DP)/MWNT/GC bioelectrode exhibited two linear responses to glucose in the concentration ranging from 0.42 μM to 8.0 mM with a correlation coefficient of 0.95, sensitivity of 52.0 $\mu AmM^{-1}\ cm^{-2}$, repeatability of 1.6% and long-term stability, which could make it a promising bioelectrode for precise detection of glucose in the biological samples.

1. Introduction

Monitoring and control of blood glucose levels is a key strategy in diabetes management [1]. In addition, detection of glucose is important for clinical diagnostics, medical validation, bioscience research and food analysis. Glucose concentration is mainly determined using enzymatic or chemical receptor techniques, but these have a limited detection range, mostly from 10^{-3} to 10^{-6} M [2–7]. Therefore, despite the extensive literature on the subject, there is still a practical requirement for an ultra-sensitive, selective, rapid and inexpensive glucose sensor with a detection limit in the micro-molar range, and which can be readily miniaturised for applications such as in-body fluids, tissue exudates, tears, sweat, calorie-controlled foods, etc. [8,9].

Efforts to develop and improve glucose sensors have continued for nearly five decades following Clark and Lyons' first report of the enzyme electrode, in 1962 [10]. One of the most challenging aspects in the development of a highly sensitive glucose sensor is the selection of a suitable enzyme immobilisation matrix, which can offer high mechanical strength, excellent conductivity and antifouling properties [11–13]. Rapid advances in the development of nano- and porous materials have vastly increased electrode surface areas and, consequently, the dynamics of interactions [14,15]. Carbon nanotube (CNT) incorporation is an extensively investigated modification to glucose enzyme electrodes, because of the excellent electron transfer capabilities of CNT as well as their large surface areas. Electropolymerisation of conducting polymers, such as polypyrrole, polyaniline, polyacetylene, polyindole, polythionine and polythiophene, has been studied extensively for the development of biosensors [16–21]. These polymers offer significant advantages due to their very good conducting and mechanical properties and good adhesion to the electrode substrate. On the other hand, non-conducting polymers could provide very thin films, due to their self-limiting growth, and hence biosensors based on these can offer fast response times. In addition, the term selectivity of non-conducting films confers improved biosensor selectivity and anti-fouling properties. Non-conducting membranes of poly phenylenediamines have been of particular interest because of their thin, dense films leading to both fast response and high H_2O_2 or O_2 selectivity. Jang et al. reported the electropolymerisation mechanism for poly(1,2-diaminobenzene) [22], and the electropolymerised poly(1,2-diaminobenzene) film was analysed by an impedimetric technique [23]. Also, GOx has been entrapped in a poly(1,2-diaminobenzene)film through the polymerisation of 1,2-diaminobenzeneon platinum-coated carbon fibres [24–26].

In the present study, an electropolymerised film of 2,6-diaminopyridine,(2,6-DAP) was prepared on the surface of a glassy carbon (GC) electrode modified with multi-walled carbon nanotubes, (MWNT),

---

* Corresponding authors at: Biosensors and Bioelectronics Centre, Department of Physics, Chemistry and Biology, IFM-Linköping University, S-58183 Linköping, Sweden. Tel.: +46 1328 2395; fax: +46 1313 7568.
E-mail addresses: makamyabi@gmail.com (M. Ali Kamyabi), ashutosh.tiwari@liu.se (A. Tiwari).

0039-9140/$ - see front matter © 2013 Elsevier B.V. All rights reserved.
http://dx.doi.org/10.1016/j.talanta.2013.07.068

in 0.1 M HCl in methanol, by cyclic voltammetry (CV). The electropolymerisation of 2,6-diaminopyridine has been studied by Morea et al., in acetonitrile solvent at a platinum electrode [27]. They described the formation of two different films depending on the deposition potential and their results revealed an electron transfer, chemical reaction, electron transfer (ECE) mechanism operating for the formation of the first film and provided evidence for nucleation and growth for the deposition of the second film. In contrast to previous work [27], we report here the electropolymerisation of 2,6-diaminopyridine on the surface of a glassy carbon (GC) electrode, in 0.1 M HCl in methanol. For the first time, we utilised the poly(2,6-DAP)/MWNT matrix to immobilise GOx as a model enzyme.

2. Experimental

2.1. Materials

The chemicals, 2,6-diaminopyridine (Sigma, 99.5%), glucose oxidase (GOx, from *Aspergillusniger*, EC 1.1.3.4. 150,000 unit/g) and glucose (Sigma, 99%) were purchased from USA and used without further purification. The multi-walled carbon nanotubes (MWNT, 1–8 nm inner diameter 2–25 nm outer diameter, 1 μm length and BET of 285 m^2/g, 99%) were obtained from the Research Institute of Petroleum Industry, Iran. Prior to use, the MWNTs were purified and functionalized by sonicating in a mixture of concentrated sulphuric and nitric acids (3:1, v/v) for about 4 h, neutralised with a large amount of de-ionized water, filtered with a millipore membrane (pore size 0.22 μm), and finally dried at 60 °C overnight. All the supplementary chemicals were of analytical grades and solutions were prepared with 18.2 MΩ deionized water. The phosphate buffer solutions (PBS) were prepared from H_3PO_4, KH_2PO_4 and K_2HPO_4 and adjusting the pH were regulated with 2 M HCl and 2.5 M KOH solutions. The supporting electrolytes were used in all the experiments with 0.1 M PBS.

2.2. Apparatus

Voltammetric experiments were performed using a Metrohm Computrace voltammetric analyser (model 757 VA). A conventional three-electrode system was used with a bare or chemically-modified GCE as working electrode, (Ag/AgCl, KCl, 3 M) reference electrode and a platinum wire counter electrode. The surface morphology of the electrodes was examined with a Hitachi S-4800 field emission scanning electron microscope (FESEM) operated at 20 kV. The specimens were sputter-coated with a thin layer of iridium (~5 nm) prior to examination. A digital pH/mV meter (mode l780 Metrohm) was applied for preparation of the buffer solution. All experiments were performed at an ambient temperature of 25 ± 2 °C. Solutions were purged with high purity nitrogen gas, (or air), for at least10 min before electrochemical measurements.

2.3. Preparation of the modified electrode

The glassy carbon electrode (2 mm diameter) was carefully polished with aluminium on polishing cloth. The electrode was placed in ethanol and subjected to vibration to remove adsorbed particles. Then 15 cycles scans were carried out in the potential range of −2.0 to +2.0 V vs. reference electrode in a solution of 1 M H_2SO_4, this process was used to remove impurities from the electrode surface [23,24]. Finally, the electrode was thoroughly washed with deionised water and dried for 5 min at 50 °C in an oven. A 10 mg of MWNT was dispersed in 10 mL dimethyl sulfoxide by ultrasonic agitation for about 30 min to give a black suspension of 1 mg/mL. The MWNT-modified electrode was prepared by casting 10 μL of the MWNT suspension on the surface of the GC electrode, which was dried in air for 4 hat 40 °C. When the dimethyl sulfoxide was volatilised, a MWNT film was formed. The surface modification of the MWNT/GCE was performed in two steps:

a) The poly(2,6-DAP) films were formed on the electrode surfaces by continuous potential cycling for 20 times between −0.3 V

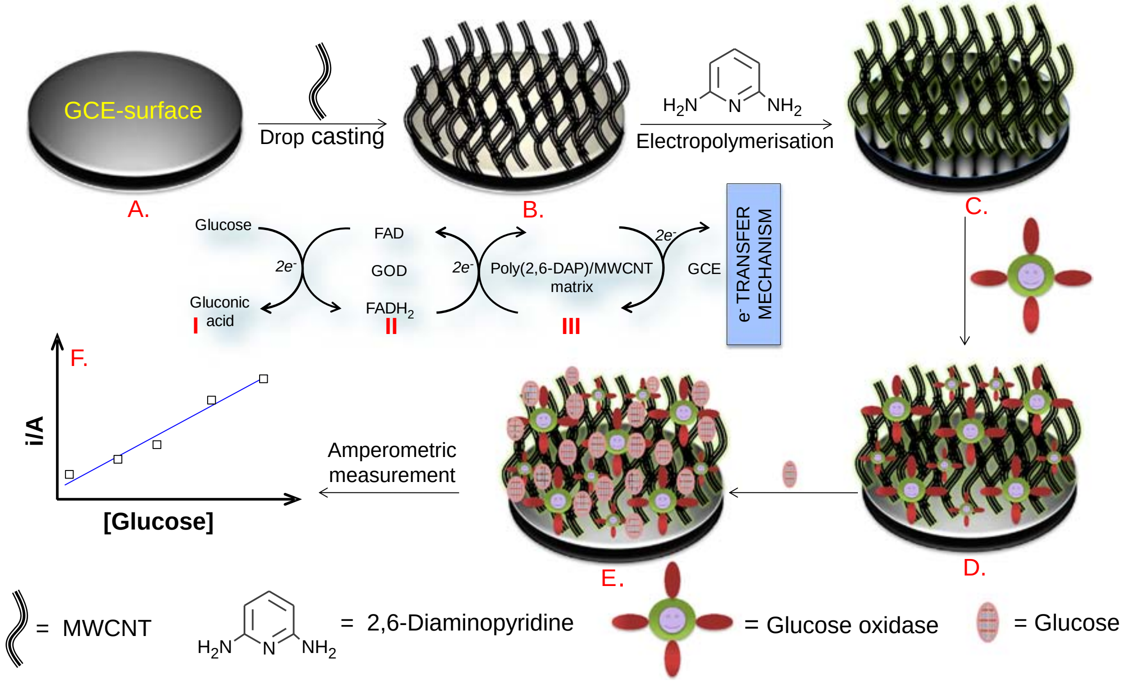

Scheme 1. Schematic illustrations of fabrication, biosensing and electron transfer mechanism of an ultra-sensitive glucose biosensor (A–F). (A–B) treatment and casting of MWNT on a GC electrode; (C) electrodeposition of poly(2,6-DAP) on MWNT/GC electrode; (D) covalent-immobilisation of GOx on a poly(2,6-DAP)/MWNT/GC electrode using glutaraldehyde as a linker and (E–F) amperometric glucose biosensing through direct electron transfer mechanism from I to III onto a GOx/poly(2,6-DAP)/MWNT/GC bioelectrode at physiological pH.

and 1.2 V at 50 mV s^{-1} in 0.1 M HCl containing 4 mM 2,6-DAP with total cell volume of 10 mL.

b) In the second step, the poly(2,6-DAP) film on the GC electrode was converted to a conducting polymer by cycling the potential scan in 0.01 M NaOH solution at the scan rate of 50 mVs^{-1} for ten times.

The surface area of the modified electrode, poly(2,6-DAP)/MWNT/GCE, was 1.053 ± 0.006 cm^2 whereas for MWNT/GCE was 0.821 ± 0.005 cm^2, which were evaluated from cyclic voltammetry experiments. After surface modification of the GCE, the modified electrode was rinsed with distilled water and stored in triply distilled water when not in use. The GOx/poly(2,6-DAP)/MWNT was prepared by dropping 5 μL of 2.5 mg/mL GOx in 0.1 M PBS of pH 5 on to the poly(2,6-DAP)/MWNT modified GCE. After drying at 4 °C in a refrigerator for 4 h, 10 μL of glutaraldehyde solution, (2.5%, w/v), was added and the electrode dried at 4 °C. Scheme 1 shows the overall fabrication of glucose biosensor from a to f that includes: (a, b) treatment and casting of MWNT on a GC electrode; (c) electrodeposition of poly(2,6-DAP) on MWNT/GC electrode; (d) covalent-assembly of GOx on a poly(2,6-DAP)/MWNT/GC electrode using glutaraldehyde as linker and (e, f) amperometric glucose biosensing via direct electron transfer mechanism from I to III. All electrodes were stored in PBS at 4 °C when not in use.

3. Results and discussion

3.1. Electrochemical study of poly(2,6-DAP): synthesis and characterisation

Prior to electropolymerisation of 2,6-DAP at the MWNT/GCE, solubility of 2,6-DAP monomer was optimised with varying concentration of HCl ranging from 0.01 to 0.1 M. The optimum solubility of 2,6-DAP was achieved with 0.1 M HCl in methanol. Continuous cyclic voltammograms were recorded using GCEs dipped in a mixture containing 4 mM of 2,6-DAP and 0.1 M HCl under deaerated condition. The effects of various factors on the formation of poly(2,6-DAP) film on the MWNT/GCE surface, such as the amount of monomer, scan rate, number of scans, potential window, pH and also the conditions of the alkaline treatment, were evaluated according to the variation of the peak current of the cyclic voltammograms (CV) obtained from the modified electrode.

Fig. 1A, displays the CV of 2,6-DAP electro-polymerisation over the range of −0.3 V to 1.2 V at 50 mV/s for 20 cycles. The forward scan of the first cycle revealed the presence of an irreversible oxidation and reduction peak of the monomer, (Fig. 1A, curve a, O_1 and R_1 peaks), with peak potentials at about 1.01 and 0.78 V vs. Ag/AgCl, respectively. In the subsequent cycles, the oxidation currents were decreased at 1.01 V with a simultaneous appearance of a pair of redox peaks at about 300–390 mV, due to the formation of poly (2,6-DAP) film. This clearly shows the oxidation of the monomer 2,6-DAP and the formation of poly(2,6-DAP) film on the surface of the MWNT/GCE. The peak-to-peak separation ($\Delta E_p = E_{pa} - E_{pc}$ of the pair redox peaks at about 300–390 mV) increased with increasing number of cycles, i.e. 90 mV in the second and 200 mV in the last cycle. This suggests that the nonconductive polymer film was formed on the surface of the GC electrode with increasing scan cycles. A similar peak was also seen for the electropolymerisation of *o*-phenylenediamine, (*o*PD) [25], and 4-nitro-1,2-phenylenediamine [26]. The electropolymerisation mechanism of 2,6-DAP monomer has been proposed in the literature [22,26,27].

The poly(2,6-DAP) is a non-conducting membrane and this modified electrode does not show any electrocatalytic activity in an aqueous solution. However, several scan cycles of the poly (2,6-DAP) film-modified GCE in an alkaline solution, (i.e., alkaline treatment), can improve the conductivity and also the electrocatalytic activity of the modified electrode. The cyclic voltammogram of MWNT/GCE modified with poly(2,6-DAP) film after alkaline treatment shows two small pairs of quasi-irreversible peaks at a formal potential of about −0.18 V, (ΔE_p = 140 mV), and −0.45 V, (ΔE_p = 60 mV), at scan rate of 50 mV in 0.1 M PBS pH 7.4 (Fig. 1B). The good conductivity and electrocatalytic activity of the modified electrode after an alkaline treatment may be due to the reduction of some of the C–N bonds in the polymer and the rearrangement of the polymer. Similar behaviour was also reported for poly(*o*-PD) [28]. Following this alkaline treatment, the resulting conductive polymeric film showed good conductivity in 0.1 M BPS, pH 7.4.

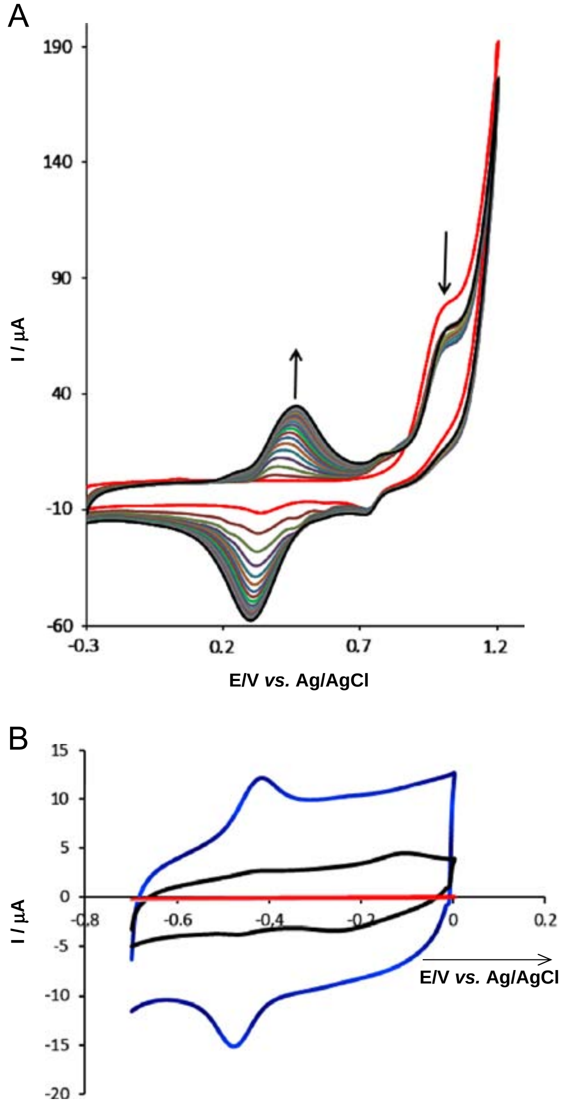

Fig. 1. (A) Cyclic voltammograms recorded during growth of poly(2,6-DAP) films on the MWNT/GC electrode in 0.1 M HCl solution containing 0.04 M of 2, 6-DAP, between −0.3 and 1.2 V vs. Ag/AgCl, 50 mVs^{-1} potential sweep rate; and 20 scan number; and (B) cyclic voltammograms for (i) GCE, (ii) the poly(2,6-DAP) film on the MWNT/GC electrode, and (iii) GOx/poly(2,6-DAP)/MWNT/GC electrode, in 0.1 M PBS at pH 7.4, between −0.3 and 1.2 V vs. Ag/AgCl, and 50 mVs^{-1} potential sweep rate.

The effect of scan rate on the CV of the poly(2,6-DAP) electrode after alkaline treatment, in the range of −0.7 V to 0.7 V in the 0.1 M PBS pH 7.4 was also investigated (Fig. S1A). The anodic and cathodic peak currents were directly proportional to the scan rate in the range below 500 mVs^{-1} with the linear equations:

I_{pa}(μA)=0.116 υ (mV s^{-1})+0.046 (n=15, R^2=0.993), I_{pc} (μA)=−0.113 υ (mV s^{-1})+4.055 (n=15, R^2=0.982) (Fig. S1B). The ratio of the anodic to cathodic peak currents obtained at various scan rates was almost unity. The formal potential $E^{0'}=(E_{pa}+E_{pc})/2$ was independent of the potential scan rate for sweep rates below 500 mV s^{-1}, suggesting a transfer coefficient of about α=0.5 for this redox reaction.

The stability of the modified electrodes without modification by GOx, and the reproducibility of their electrochemical behaviour were investigated by cyclic voltammetry after storing them in buffer solution at pH 7.4 for up to two week and then recording the CVs. After immersing the modified electrodes for 24 h, the currents and the potential response remained more or less unchanged. The recorded CVs after two weeks storage under ambient conditions were reproducible and unchanged. In addition, the stability and reproducibility of the modified electrodes were examined by repetitive recording of the CVs in buffer solution at pH 7.4. There was no change in the peak height and peak-to-peak separation after 50 cycles of repetitive cycling at scan rate of 100 mVs^{-1}.

3.2. Immobilisation of enzyme and electrocatalytic activity of enzyme-modified electrode

The GOx enzyme was covalently immobilised on the poly(2,6-DAP)/MWNT/GC electrode surface by cross-linking with glutaraldehyde. Initially, GOx was immobilised on the surface of the poly (2,6-DAP)/MWNT/GC electrode and after drying, glutaraldehyde was added as a linker, as described in the literature [29]. The resulting enzyme electrodes were stored at 4 °C in a refrigerator (in air) when not in use.

Fig. 1B shows the CVs obtained at (i) bare GC, (ii) poly(2,6-DAP)/MWNT/GC and (iii) GOx/poly(2,6-DAP)/MWNT/GC electrodes in deoxygenated PBS at the scan rate of 50 mV s^{-1}. Cyclic voltammograms were recorded in the potential range of −0.7 to 0.0 V. A pair of well-defined redox peaks was observed at GOx/poly(2,6-DAP)/MWNT modified GCE in the same potential window. The $E^{0'}$ associated with this redox couple is 0.44 V, which is close to the $E^{0'}$ of other GOx-modified electrodes reported previously [30,31]. The peak-to-peak separation (ΔE_p) is about 30 mV. This redox couple is thus consistent with previously reported direct electron transfer of GOx at similarly modified GCE surfaces.

To indicate the effects of MWNTs and the polymer on the responses of the sensor, the following combination of the modified electrode were also studied: (i) GOx/poly(2,6-DAP)/GCE and (ii) GOx/MWNT/GCE. The results revealed that in both cases there were poor linear ranges and sensitivities for glucose.

Fig. 2A shows the cyclic voltammograms of glucose oxidase/poly(2,6-DAP)/ MWNT-modified GC electrode in pH 7.4 at different scan rates ranging from 40 to 500 mV s^{-1}. Both the anodic and cathodic peaks currents are linearly proportional to the scan rate in the range of 10–200 mVs^{-1}, indicating a surface controlled electrode process (Fig. 2B). Moreover, redox potentials were almost the same at the different scan rate. It is clear that GOx adsorbed onto the surface undergoes a reversible electron transfer with the modified electrode. The formal potential $E^{0'}=(E_{pa}+E_{pc})/2$ is almost independent of the potential scan rate for sweep rates below 200 mV s^{-1} and the peak to peak separation is about 35 mV

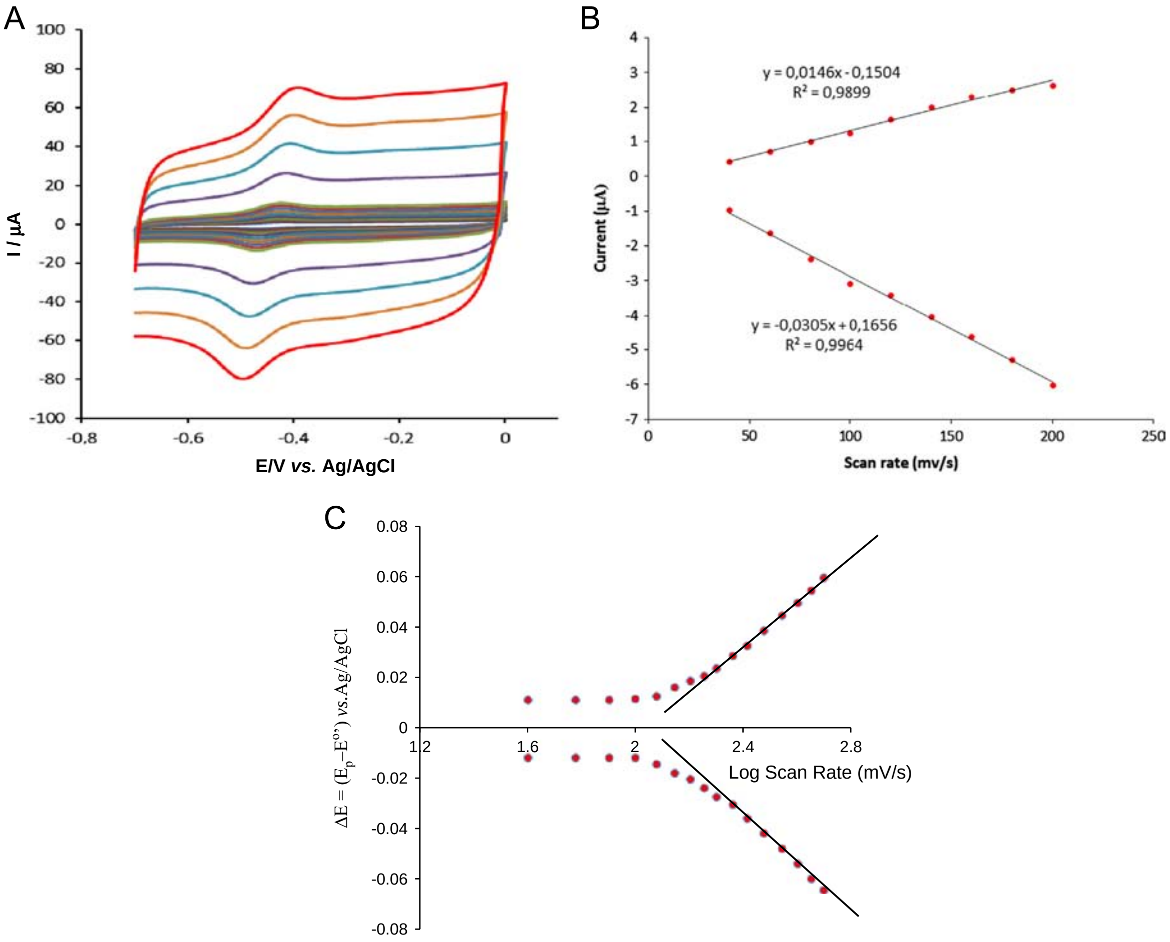

Fig. 2. (A) Cyclic voltammograms of GOx/poly(2, 6-DAP)/MWNTs/GC electrode in PBS of 7.4 pH at different scan rates ranging from 40 to 500 mVs^{-1}, (B) plot of anodic and cathodic peak current vs. scan rate, and (C) plots of peak potential separations vs. log scan rates.

at scan rates below 200 mV s^{-1}, suggesting facile charge transfer kinetics over this range of sweep rates. On the other hand, it was found that at scan rates of above 200 mV s^{-1}, ΔE_p increased with increasing scan rate. The values of peak-to-peak potential separations are proportional to the logarithm of the scan rate (Fig. 2C). Based on the Laviron theory, the transfer coefficient (α) and electron transfer rate constant (K_s) can be estimated by measuring the variation of peak potential with scan rate [30]. The transfer coefficient and heterogeneous electron transfer rate constant were approximately 0.6 and 4.0 s^{-1}, respectively. This value for electron transfer rate constant is comparable with the apparent heterogeneous electron transfer rate constant reported previously [26,27].

3.3. Morphological characteristics of the modified electrodes

Typical SEM pictures of the poly(2,6-DAP)/MWNT/GC and GOx/poly(2,6-DAP)/MWNT/GC electrodes are shown in Fig. 3. Fig. 3A shows the porous and three-dimensional surface of poly(2,6-DAP)/MWNT/GC electrode. The porous surface of the poly(2,6-DAP)/MWNT/GC electrode provided a large surface-to-volume ratio, which was able to accommodate large amounts of active GOx on the electrode. Further, this enhanced enzyme stability and direct electron transfer between the active site of enzyme on the poly(2,6-DAP)/MWNT/GC electrode. Immobilisation of GOx on the poly(2,6-DAP)/MWNT/GC electrode resulted in a homogeneous globular surface morphology (Fig. 3B). The uniform globule-like bioelectrode may be formed due to a good cross-linking of GOx by glutaraldehyde on the surface of the poly(2,6-DAP)/MWNT/GC electrode.

3.4. Effect of pH

Fig. 4 shows the effect of pH on the GOx ($FAD/FADH_2$) redox couple at GOx/poly(2,6-DAP)/MWNT-modified GC electrode in various buffer solutions (pH 2–10). The redox peak current remained stable in the pH range 2–10. The redox couple was also reproducible when the composite film-modified GCE was transferred from one buffer solution to another. The influence of pH over the anodic peak potential, (E_{pa}), of $FAD/FADH_2$ redox couple at GOx/poly(2,6-DAP)/MWNT-modified GCE is shown in Fig. 4B. From the plot of $E^{0'}$ vs. pH, it is apparent that both E_{pa}, E_{pc} and $E^{0'}$exhibited a linear dependence over different pHs. The correlation coefficient was 0.994 and the slope was −54 mV/pH, which is close to the theoretical value of Nernstian equation for equal number of proton and electron transfer process [32]. Thus the $FAD/FADH_2$ redox couple reported in this study comprises an equal number of protons and electrons transfer processes as shown in Scheme 1 (cf., I–III).

3.5. Electrocatalysis of GOx/poly(2,6-DAP)/MWNT-modified GCE towards oxygen reduction and glucose determination

The influence of dissolved oxygen on the GOx/poly(2,6-DAP)/MWNT-modified GCE was investigated in deoxygenated and oxygenated PBS (Fig. 5). From the results it is obvious that the reduction peak current observed at the modified GCE in oxygenated PBS (Fig. 5A) was considerable. This result reveals that dissolved oxygen was reduced effectively at the GOx/poly(2,6-DAP)/MWNT-modified GCE. Similar observations have been reported at GOx modified electrodes [30,33,34]. Furthermore, the electrocatalytic response of the modified GC electrodes towards glucose was compared under both deoxygenated and oxygenated PBS conditions. Upon addition of glucose to air-saturated PBS, the reduction current response of GOx/poly(2,6-DAP)/MWNT-modified GCE decreased (Fig. 5A). The decrease increased with increasing glucose concentrations. Also the current at positive potentials (about 0.2 V vs. Ag/AgCl) was increased with addition of glucose, whereas there was no effect in the voltammogram of GOx/poly(2,6-DAP)/MWNT-modified GCE's with the addition of glucose in to the deoxygenated PBS condition. The results revelled that only some parts of the immobilised GOx maintained its bioactivity and apparently kept its native structure on the surface of the modified electrode after the modification. It led to work as the first generation of glucose sensor (i.e., amperometric detection of glucose by the production of hydrogen peroxide under oxygenated condition). FADs groups were appeared from denatured GOx on the surface of electrode via catalysed reduction of oxygen.

The concentration of the oxidised form of FAD on electrode surface should decrease in the presence of substrate, glucose. Thus, the addition of glucose restrained the electrocatalytic reaction and led to the decrease in the reduction current. Fig. 5B shows a plot of peak current decrease vs. glucose concentration. The calibration range of glucose concentration was studied from 4.2×10^{-7} to 8×10^{-3} M. Linear response ranges to glucose concentration were obtained of 0.42–89 μM and 0.9–8.0 mM, with correlation coefficients of 0.95 and a detection limit of 0.13 μM at a signal-to-noise ratio of three. The sensitivity of GOx/Au/CPE to glucose was found to be 52.0 μA mM^{-1} cm^{-2}. Further, Fig. 5A shows the current at positive potentials (about 0.2 V vs. Ag/AgCl) increased on addition of glucose. Hydrogen peroxide produced under oxygenated conditions

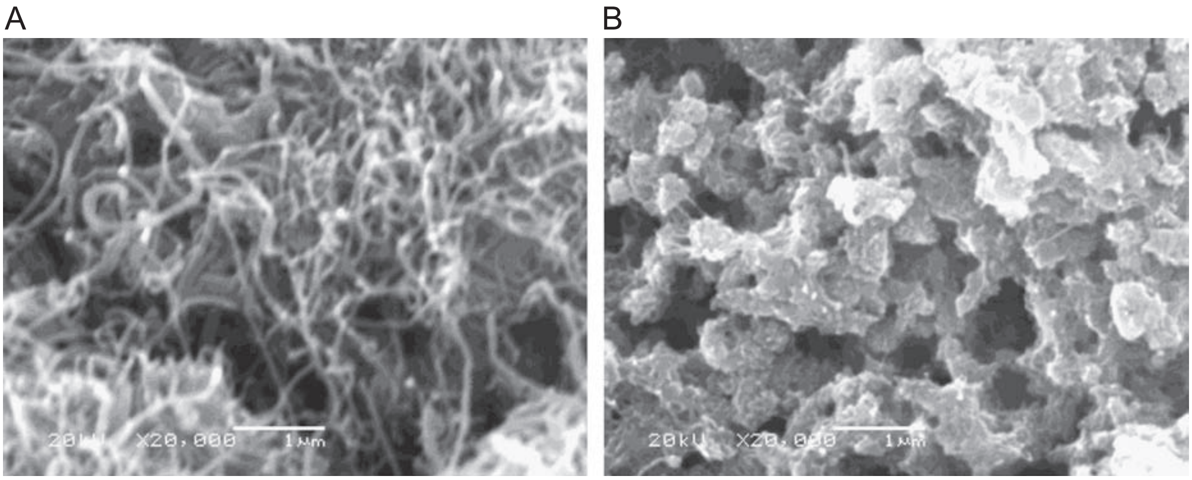

Fig. 3. SEM images of the (A) poly(2,6-DAP)/MWNT/GC and (B) GOx/poly(2,6-DAP)/MWNT/GC electrodes.

is oxidised at these potentials resulting in an increased anodic current. The calibration curve was linear over the concentration range 1.66×10^{-4} to 8.33×10^{-3} M, with a correlation coefficient of 0.983. The apparent Michaelis–Menten constant K_m of the biosensor can be calculated from the Lineweaver–Burk equation: $1/I_{ss}=(K_m/I_{max})(1/C_g)+1/I_{max}$, where C_g is the substrate concentration, I_{ss} is the steady-state current and I_{max} is the maximum current measured under substrate saturation (i.e., not shown). From the curve of the $I_{ss}{}^{-1}$ versus $C_g{}^{-1}$, based on the experimental data from Fig. 5B, the apparent Michaelis–Menten constant K_m was estimated to be 0.20 mM.

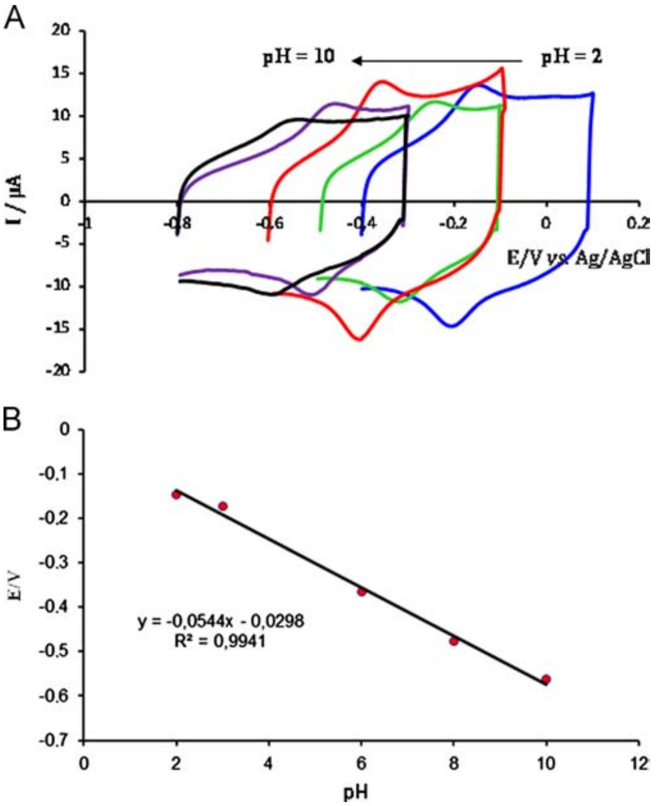

Fig. 4. (A) Cyclic voltammograms of GOx/poly(2, 6-DAP)/MWNT/GC electrode at different pH 2, 4, 6, 8 and 10, 100 mVs^{-1} scan rates and (B) dependence of the oxidation peak potentials of GOx/poly(2,6-DAP)/MWNT/GC electrode on pH in 0.1 M buffer solution at varying pH ranging from 2 to 10.

Table 1 compares the characteristics of the new glucose biosensor based on the GOx/poly(2,6-DAP)/MWNT-modified GC electrode with those reported in the literature. It is apparent that the present GOx/poly(2,6-DAP)/MWNT-modified GCE glucose biosensor possesses wider range of detection, i.e. from 0.42–89 µM and from 0.9 to 8.0 mM, a longer shelf life and higher sensitivity.

3.6. *Reproducibility, stability and sample analysis*

Storage and operational stabilities are important considerations for an immobilised enzyme. When the enzyme electrode was stored at 4 °C, it retained 93% of its initial current response for glucose after intermittent use over a 10 day period and in 30 successive measurements, the response of the electrodes did not change significantly. The operational stability of the biosensors was also examined using continuous cyclic voltammetry. When 200 continuous cyclic scans were performed in the potential range from −0.7 to 0.0 V with a 100 mV/s scan rate, only a 3% decrease in the response was detected, demonstrating good operational stability. The results suggest that the use of a direct electron transfer mechanism with GOx results in higher stability and should deliver acceptable fabrication precision. The relative SD was ±1.6% for 10 successive determination of 1.2×10^{-5} M of glucose and the fabrication reproducibility of eight electrodes, made independently, showed a relative SD of ±7.6% for the current determination at a glucose concentration of 1.2 ± 10^{-5} M.

3.7. *Specificity and interferences*

GOx possesses high specific catalytic activity towards the glucose even in the presence of other carbohydrates [45]. The main interferences in enzyme electrodes result from electroactive species diffusing to the sensor surface. To evaluate the selectivity of the GOx/poly(2,6-DAP)/MWNT-modified GCE biosensor, the effect of the presence of the possible interfering substances like uric acid, (UA), dopamine, (DA), ascorbic acid (AA) and also acetaminophen, on the cyclic voltammetric current of the proposed biosensor in 1 mM glucose was investigated. A 5% error criterion was adopted. No significant interference was observed for UA, DA and AA at concentration of 0.5 mM UA, DA and AA.

3.8. *Biological samples*

Blood serum samples were collected from a nearby clinical laboratory and tested for glucose concentration with the developed

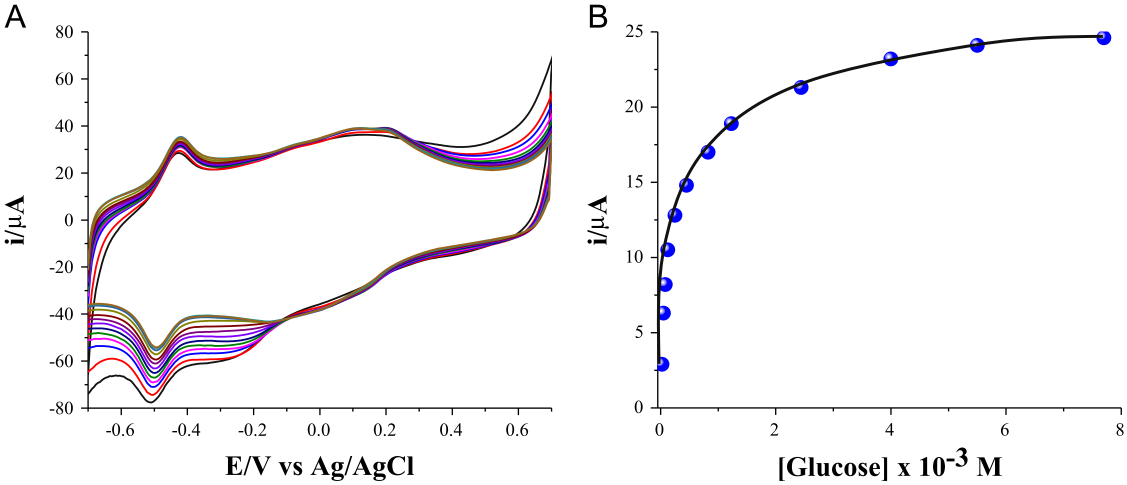

Fig. 5. (A) Cyclic voltammograms of GOx/poly(2,6-DAP)/MWNT/GC electrode in the 0.1 M PBS of pH 7.4 with glucose concentrations ranging from 4.16×10^{-9} to 8×10^{-3} M at 100 mVs^{-1} scan rate and (B) the calibration curve of cyclic voltammograms A.

Table 1
Comparison of electroanalytical values for glucose oxidation at various direct electron transfer GOx modified electrodes.

Film type	Sensitivity	K_s (s^{-1})	K_m	LDR	Stability		Rejection of interferences	Ref.
					Cycles	Days		
Nafion-GOx-CNT/GCE	–	1.53	–	–	–	–	–	[17]
GOD/CNTs/CS/GCE	0.52 μAmM^{-1}	7.73	8.2 mM	0–7.8 mM	50 (no significant decrease)	15 (no significant decrease)	AA/L-Cys/ acetaminophen	[19]
	89.035 μAmM^{-1}			40 mM			AA/UA/AP	[20]
GOx/CNT mat/wire	4.05 μA mM^{-1} cm^{-2}	1.72	2.18 mM	0.2–2.18 mM	–	–	–	[21]
Au NPs/GOx-CNTs-PVA/ GCE	16.6 μA mM^{-1} cm^{-2}	2.2	–	0.5–8 mM	–	30 (decrease slightly)	UA/AA/L-Cys/ Ca^{+2}/Mg^{+2}/Cl^{-}	[35]
GOx/GR-TiO_2/GCE	6.26 μA mM^{-1} cm^{-2}	–	–	0-8 mM	–	–	UA/AA	[36]
GOx/OMC-Au/GCE	4.34	5.03	0.6 mM	0.05–0.3	50 (no significant decrease)	30 (88% initial response)	UA/AA	[37]
	0.96 μAmM^{-1}			0.3–20 mM				
GOx/Au/GCE	–		15.6μM	2.5–32.5 60–130 μM	–	7 (94.6% initial response)	AA/L-Cys	[38]
GAD/GOx/GCNT/GCE	2.47 μA mM^{-1} cm^{-2}	1.08	–	6.30–20.09 mM	–	14 days in PBS (96.37% initial response)	AA/UA/DA/AP/ LA/PA	[39]
GOx/CNTs-DHP/GCE	–	1.69	–	0.02–15 mM	–	30 (89% initial response)	L-Cys	[40]
($GOx/ConA)_3$/Pt nano-CNTs/GCE	--	5.09	0.94 mM	1.2×10^{-6}–2.0×10^{-3} M	100 (96.4% initial response)	10 (94.4% initial response)	AA/UA/Cys/AP	[41]
GOx/ZnO/GOx/CNTs/GCE	10.03μA mM^{-1} cm^{-2}	1.98	2.48 mM	6.67×10^{-6}–1.29×10^{-3} M	–	10 (94.6% initial response)	AA/L-Cys/DA/Gly	[42]
GOx/PPMH/GCE	–	1.32	0.64 mM	Up to 2 mM	–	–	–	[43]
GOx/PMB@SiO_2 nano/ GCE	–	2.44	0.5 mM	0.01–1.11 mM	–	14 (92% initial response)	UA/AA	[44]
GOx/Poly 2,6 di-amino-pyridine/MWNTs/GCE	**52.0 μA** mM^{-1} **cm**$^{-2}$ **0.78 μA** mM^{-1}**cm**$^{-2}$	**4.0**	**0.22** mM	**4.16×10^{-4}–1.20×10^{-1}** mM **0.9–8.0** mM	**200** (97% initial response)	**10** (93% initial response)	**AA/UA/DA/AP**	**This work**

LDR, linear dynamic range; CNTs, carbon nanotubes; GCE, glassy carbon electrode; AP, acetaminophen; LA, lactate; Gly, glycine; PA, pyruvate; Ordered mesoporous carbon–Au nanoparticles (OMC–Au); GAD, glutaraldehyde; GCNT, gelatin-multiwalled carbon nanotube; PVA, polyvinyl alcohol; GR, graphene; PPMH, poly-1,10-phenanthroline; PMB, poly(methylene blue).

sensor. The determination of glucose was performed on the sensor utilising the standard addition method. After the current response was determined in 5.0 ml of 0.1 M pH 7.4 PBS containing sample of 20 µL, which depended on the concentration of glucose, four 10 µL, 20 µM glucose solutions were successively added to the system for standard addition determination. All the concentrations of glucose in detection solutions were in the linear response range. The glucose level was determined to be 15.86 ± 0.15 mM, which was close to the value of 16.04 mM obtained by spectrophotometry, suggesting that the proposed sensor can be used for the determination of glucose level in biological fluids.

4. Conclusion

GOx was efficiently immobilised on a new poly(2,6-DAP)/MWNT/GC electrode. Some parts of the immobilised GOx maintained its bioactivity and apparently keeps its native structure. The reduced form of the released FAD groups of enzyme could be oxidised by dissolved oxygen to produce an electrocatalytic reaction, which was restrained by glucose, due to the reaction between the oxidised form of GOx and its substrate. This novel sensor displayed high sensitivity (52.0 µA mM^{-1} cm^{-2}) and linear ranges between 0.42–89 µM and 0.9–8.0 mM for glucose were observed. The electrode appeared to be relatively immune to electrochemical interferences. The apparent Michaelis–Menten constant was calculated to be 0.20 mM. Given its convenient preparation, excellent properties and nanomole detection limit, this biosensor should be particularly suitable for the new generation of ultra-miniaturised glucose sensors envisaged for glucose determination in tissue exudates.

Acknowledgements

The authors wish to express their gratitude to the European Commission (PIIF-GA-2009-254955), LIST – Linköping University and Zanjan University Research Council for the financial supports of this work.

Appendix A. Supporting information

Supplementary data associated with this article can be found in the online version at http://dx.doi.org/10.1016/j.talanta.2013.07.068.

References

[1] J.D. Newman, A.P.F. Turner, Biosens. Bioelectron. 20 (2005) 2435.
[2] J. Wang, Chem. Rev. 108 (2008) 814.
[3] E. Murphy-Pérez, S.K. Arya, S. Bhansali, Analyst 136 (2011) 1686.
[4] Y. Degani, A. Heller, J. Phys. Chem. 91 (1987) 1285.
[5] X. Qin, W. Lu, Y. Luo, G. Chang, A.M. Asiri, A.O. Al-Youbi, X. Sun, Analyst 137 (2012) 939.
[6] Y. Chen, Y. Li, D. Sun, D. Tian, J. Zhang, J.-J. Zhu, J. Mater. Chem. 21 (2011) 7604.
[7] S. Bao, C.M. Li, J. Zang, X. Cui, Y. Qiao, J. Guo, Adv. Funct. Mater. 18 (2008) 591.
[8] A. Tiwari, M. Ramalingam, H. Kobayashi, A.P.F. Turner, Biomedical Materials and Diagnostic Devices, Wiley-Scrivener, USA, 2012.
[9] J. Wang, Talanta 75 (2008) 636.
[10] L.C. Clark Jr., C. Lyons, N.Y. Ann., Acad. Sci. 102 (1962) 29.
[11] M.M. Rahman, A.J.S. Ahammad, J.-H. Jin, S.J. Ahn, J.-J. Lee, Sensors 10 (2010) 4855.
[12] A. Tiwari, D. Terada, P.K. Sharma, R.K. Dutta, C. Yoshikawa, A.C. Pandey, H. Kobayashi, Anal. Methods 3 (2011) 217.
[13] J. Wang, Chem. Rev. 108 (2008) 814.
[14] A. Tiwari, S.R. Dhakate, Int. J. Biol. Macromol. 44 (2009) 408.
[15] A. Tiwari, S. Gong, Electroanalysis 20 (2008) 2119.

[16] Y. Oztekin, A. Ramanaviciene, Z. Yazicigil, A.O. Solak, A. Ramanavicius, Biosens. Bioelectron. 26 (2011) 2541–2546.

[17] X. Xiao, B. Zhou, L. Zhu, L. Xu, L. Tan, H. Tang, Y. Zhang, Q. Xie, S. Yao, Sens. Actuators B 165 (2012) 126–132.

[18] B. Haghighi, M.A. Tabrizi, Colloids and Surfaces B, Biointerfaces 103 (2013) 566–571.

[19] Y.-C. Tsai, S.-C. Li, S.-W. Liao, Biosens. Bioelectron. 22 (2006) 495–500.

[20] J.-C. Vidal, Microchim. Acta 143 (2003) 93.

[21] M. Gerard, A. Chaubey, B. Malhotra, Biosens. Bioelectron. 17 (2002) 345.

[22] V. Saxena, B.D. Malhotra, Curr. Appl. Phys. 3 (2003) 293.

[23] D.-H. Jang, Bull. Korean Chem. Soc. 16 (1995) 392.

[24] K. Martinusz, G. Ling, G. Inzelt, J. Electroanal. Chem. 433 (1997) 1.

[25] M. Somasundrum, K. Aoki, J. Electroanal. Chem. 530 (2002) 40.

[26] A. Griffith, A. Glidle, J.M. Cooper, Biosens. Bioelectron. 11 (1996) 625.

[27] T. Yao, Anal. Sci. 19 (2003) 61.

[28] G. Morea, A. Guerrieri, C. Malitesta, L. Torsi, J. Chem. Soc. Faraday Trans. 87 (1991) 3515.

[29] A. Tiwari, S. Deshpande, H. Kobayashi, A.P.F. Turner, Biosens. Bioelectron. 35 (2012) 224.

[30] P.R. Solanki, A.K. Kausik, A.A. Ahamad, A. Tiwari, B.D. Malhotra, Sens. Actuators B 137 (2009) 727.

[31] A. Salimi, E. Sharifi, A. Noorbakhsh, S. Soltanian, Biosens. Bioelectron. 22 (2007) 3146.

[32] N. Jia, L. Liu, Q. Zhou, L. Wang, M. Yan, Z. Jiang, Electrochim. Acta 51 (2005) 611.

[33] D. Wen, Y. Liu, G. Yang, S. Dong, Electrochim. Acta 52 (2007) 5312.

[34] R. Garjonyte, A. Malinauskas, Sens. Actuators B 56 (1999) 85.

[35] H. Zhang, Z. Meng, Q. Wang, J. Zheng, Sens. Actuators B 158 (2011) 23.

[36] H. Dong Jang, S.K. Kim, H. Chang, K. Roh, J. Choi, J. Huang, Biosens. Bioelectron. 38 (2012) 184.

[37] L. Wang, J. Bai, X. Bo, X. Zhang, L. Guo, Talanta 83 (2011) 1386.

[38] C. Qiu, X. Wang, X. Liu, S. Hou, H. Ma, Electrochim. Acta 67 (2012) 140.

[39] A.P. Periasamy, Y.-J. Chang, S.-M. Chen, Bioelectrochemistry. 80 (2011) 114.

[40] B.C. Janegitz, R. Pauliukaite, M.E. Ghica, C.M.A. Brett, O. Fatibello-Filho, Sens. Actuators B 158 (2011) 411.

[41] W. Li, R. Yuan, Y. Chai, H. Zhong, Y. Wang, Electrochim. Acta 56 (2011) 4203.

[42] F. Hu, S. Chen, C. Wang, R. Yuan, Y. Chai, Y. Xiang, C. Wang, J. Mol. Catal. B: Enzymatic 72 (2011) 298.

[43] Y. Oztekin, A. Ramanaviciene, Z. Yazicigil, A.O. Solak, A. Ramanavicius, Biosens. Bioelectron. 26 (2011) 2541.

[44] X. Xiao, B. Zhou, L. Zhu, L. Xu, L. Tan, H. Tang, Y. Zhang, Q. Xie, S. Yao, Sens. Actuators B 165 (2012) 126.

[45] R. Wilson, A.P.F. Turner, Biosens. Bioelectron. 7 (1992) 165.